Jurnal Kejuruteraan 36(1) 2024: 233-248
https://doi.org/10.17576/jkukm-2024-36(1)-22

CFD Investigation of Methane Combustion with Excess Air in Can-Type Gas Turbine Combustor

Md Shamsuzzaman Zahir[a], Hasril Hasini[a,b *], Nur Irmawati Om[a,b], Byan Wahyu Riyandwita[c] & *Norfadilah Mansyur*[b]

[a] *Department of Mechanical Engineering, College of Engineering, Universiti Tenaga Nasional, Jalan IKRAM-UNITEN, 43000 Kajang, Selangor, MALAYSIA*

[b] *Institute for Sustainable Engineering, Universiti Tenaga Nasional, Jalan IKRAM-UNITEN, 43000 Kajang, Selangor, MALAYSIA*

[c] *Department of Mechanical Engineering, Universitas Pertamina, Jalan Teuku Nyak Arief, Simprug Jakarta 12220, Indonesia*

**Corresponding author: hasril@uniten.edu.my*

Received 15 May 2023, Received in revised form 22 June 2023
Accepted 22 July 2023, Available online 30 January 2024

ABSTRACT

This paper presents an investigation on the effect of excess air to combustion characteristics in a full-scale, gas turbine combustor, commonly used in power plant. The investigation was carried out using Computational Fluid Dynamics (CFD), and prior validation was made with the actual operation data of a power station, as well as the adiabatic flame temperature of methane. The mass fraction of CO_2, O_2 and NO_x emissions for blended methane with different percentages of excess air explosions was also investigated. The stoichiometric excess air varies from 0% to 30% with air-fuel mixture of 2.7 kg/s. The geometric model of the combustor is extracted from actual gas turbine combustor using 3D scanner and converted into CAD model for simulation. The Navier-Stokes equations were solved using commercial CFD code, ANSYS Fluent, with RNG k-ε chosen to close the turbulence. For reacting species, the species transport model is assumed. Results showed that the addition of excess air during combustor has little effect on the velocity and temperature distribution, both at the combustor interior, as well as at the exit. For the emission of CO_2 and O_2, though there was no clear trend on the relations between the emission of these species and the excess air, the impact was quite significant. The production of NO_x was also found to be independent on the excess air ratio, but instead, was a strong function of combustion and exhaust gas temperature.

Keywords: CFD, methane, excess air, species transport, CO_2, O_2, NO_x

INTRODUCTION

It is widely known that burning fossil fuels releases gases that raise the earth's average temperature and cause environmental pollution, storms, floods, and other disasters (Tamang et al. 2022). This problem is becoming more prominent in the current decade with the uncertainties in the supply of conventional or carbon-based fuels. A lot of efforts have been given to enhance renewable energy technologies as replacement to conventional power generation. However, for electricity supply stability consideration, many countries around the world still depend on fossil-fuels especially coal as the main source of energy. As consideration to minimizing CO_2 emission, efforts are also put to find ways to clean up emissions from these fuels (Beddu et al. 2022).

For gas turbine power station, most of the cases, the gas turbine (GT) uses conventional fuel to run, which is natural gas. The fuel cost is relatively expensive. Furthermore, the pricing of conventional fuel, such as natural gas is always fluctuating, with an increasing trend. These uncertainties cause hike in the electricity price. Technological advancement of gas turbine and its key components are accelerating at a fast rate and at present, it is closed

to saturation. The majority of the work done in the field of gas turbine combustion focused on the pollutants emitted during GT operation using conventional fuels. Ezekiel (2015) produced a training handbook on internal combustion (IC) engines and noted that GT is the best option for producing electricity by firing natural gas. Mechanical energy is transformed into electric power because of its high operational speed, lower lubrication and operational cost, durability, efficiency, flexibility, and environmentally friendly. The function of a combustor of a gas turbine is to provide energy to the system to power the turbines which later create high-velocity, high-temperature exhaust. Combustion chambers must be built to provide steady combustion of the injected fuel and optimal fuel usage within the space constraints and throughout various air-to-fuel ratios.

A combustor must confine and sustain stable combustion despite extremely high air flow rates. Combustion chambers are accurately designed to combine and ignite the air and fuel before adding additional air to complete the combustion process (Kumar et al. 2016). Li et al. (2019) built a combustor of a single swirl with a low calorific value and discovered that optimizing inlet air distribution resulted in reduced emission through experimentation and modelling. The impact of an air distribution method on a micro combustor was explored. Yan et al. (2021) discovered that when the airflow on the cavity wall near the recirculation zone rose, the high-temperature region and OH content steadily rose. Abdul Rahman et al (2021) carried out investigation on combustion characteristics in a micro channel combustor and reported that the slit gap had significant influence to the combustion behavior. Xiao et al. (2019) did a numerical study of 7 different methods for setting the dilution holes in a GT combustor. It was shown that changing the fluid velocity significantly impacted the fuel efficiency and flow characteristics but had little effect on the overall pressure coefficient. Methane-air combustion is likely the most well-known mixture used in a GT combustor. It consists of 325 chemical reactions and 53 species by the GRI-Mech 3.0 mechanism, Smith et al. (2022). This mechanism was developed to simulate natural gas combustion, including NO production and re-burn chemistry.

Progress in GT combustion research includes the study of viability of using carbon-free fuels such as hydrogen and ammonia. An investigation of methane and ammonia combustion in a micro gas turbine (MGT) was made at different temperature loads where CH_4 and NH_3 are considered carbon-free alternative fuels that can minimize environmental pollution (Tian et al. 2009, Okaforet al. 2020 and Woo et al. 2016). The high-temperature zone of the NH_3/air flame moves toward the combustion chamber's exit more quickly than that of the CH_4/air flame and was 2.89 times higher than those from CH_4/air flame (Wang et al. 2022).

Zeng et al. (2022) studied natural gas combustion and emission characteristic of heavy-duty GT using the method of constant volume ignition reactor, chemical shock tube, GRI 3.0, USC 2.0 and NUI Galway models. Ghenai et al. (2010) numerically tested syngas combustion using a can-type combustor model where the hydrogen fuel mixture was from 0% to 100%. The results revealed that the fuel's hydrogen enrichment dramatically impacted the mixture fraction, flow structure and combustion properties. Due to the lower quantity of carbonaceous fuel, the hydrogen-enriched fuel can also minimize emissions of CO and CO_2. Liu et al. (2012) numerically investigated oxy-fuel (CH_4, O_2, CO_2 and H_2O) in GT combustor using thermodynamic calculation and chemical kinetic. The numerical estimates indicate that, for oxy-fuel combustion, there was a range of oxygen/diluent ratios within which flames were stable and emitted low levels of unburned intermediates. The most significant cause of emissions of CO_2 in the future decades will be from fossil-fuel-based, big power plants.

Nemitallah et al. (2012), Shakeel et al. (2018) and Mahmoud et al. (2018) conducted a computational analysis to study the combustion properties of oxy-methane in a GT combustor. The results showed that the energy level, oxidizer mixture (CO_2), and equivalency ratio affected combustion characteristics and CO emission rate. Jiang et al (2020) and Yu et al. (2021) numerically investigated the effects of the upstream strut and the trapezoidal in co-axial supersonic airflow for jet fuel injection. The results showed that a trapezoidal strut increased fuel mixing by around 18% compared to a rectangular strut. Moreover, an upstream strut with big space jets improved total fuel/air mixing by 15%.

A number of works were dedicated to explore alternative fuels for substituting the conventional, carbon-based fuels, which emit huge amount of CO_2. Though the alternative fuels can produce reasonable amount of heat per kg, there are other means that can be adopted by power plant operators to improve efficiency. Among others are to control operating parameters such as the fuel and air flow rate, swirl air and air fuel ratio. This work aims to investigate the effect of air fuel ratio, or excess air to the combustion behaviour in a can combustor.

METHODOLOGY

Figure 1 summarizes the methodology used in this work. The modelling of the full-scale gas turbine combustor involves first, the scanning of the combustor on-site during overhaul. Conversion of

the data into readable CAD model was done via Solidworks. A three-dimensional scan of a thermal power plants can-type combustor yields its detail shape. The scanned data was translated into typical CAD data for cleaning and exported to readable information in FLUENT. Prior to the simulation, the combustor domain is meshed, and optimization of the cell number is made to ensure grid independent solutions. Flow and combustion characteristics were solved using commercial CFD code, FLUENT.

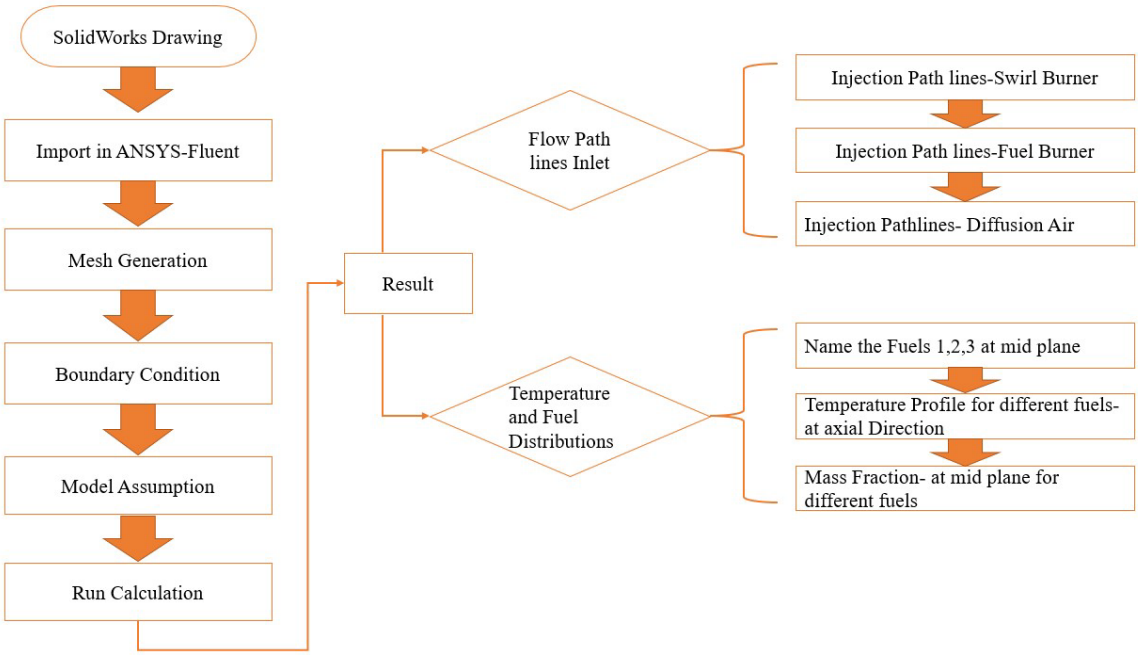

FIGURE 1. Summary of the methodology used in the present work

Governing Equations

The air flow and combustion reaction inside the combustor can be modelled using steady Reynolds Average Navier-Stokes (RANS) equations. The general continuity, momentum and energy equations are given by Eq. 1 and Eq. 2 respectively as follows:

$$\frac{\partial}{\partial x_i}(\rho \bar{u}_i) = 0 \qquad (1)$$

$$\frac{\partial}{\partial x_j}(\rho \bar{u}_i\, \bar{u}_j) = -\frac{\partial \bar{p}}{\partial x_i} + \frac{\partial}{\partial x_j}\left[(\mu + \mu_T)\left(\frac{\partial \bar{u}_i}{\partial x_j} + \frac{\partial \bar{u}_j}{\partial x_i}\right) - \frac{2}{3}\rho k \delta_{ij} - g_i(\rho - \rho_0)\right] \qquad (2)$$

Turbulence effect in the mean flow variables is considered as in Eq. 2. The buoyancy term is also included in this equation to account for density variations of the air. In CFD calculation, the RANS equations were solved using the SIMPLE algorithm. The flow of air is assumed to follow the ideal gas behaviour with constant air properties. The energy equation is described as follows:

$$\frac{\partial}{\partial x_i}(\rho c_p\, \bar{T} \bar{u}_i) = \frac{\partial}{\partial x_i}\left[(\lambda + \lambda_T)\frac{\partial \bar{T}}{\partial x_i}\right] \qquad (3)$$

The mixture fraction is resolved using the following equation:

$$\frac{\partial(\overline{\rho f u_j})}{\partial x_j} = \frac{\partial\left[\left(\frac{\mu_t}{\sigma_t}\right)\frac{\partial \bar{f}}{\partial x_j}\right]}{\partial x_j} + S_m \qquad (4)$$

The mass fraction f is written in terms of elemental mass fraction as:

$$f = \frac{Z_k - Z_{k,O}}{Z_{k,F} - Z_{k,O}} \qquad (5)$$

Where Z_k is the mass fraction of element k and subscripts F and O denote fuel and oxidizer, respectively.

The combustion model was based on eddy dissipation model which computes the rate of reaction under the assumption that the chemical kinetics are fast compared to the rate at which the reactants are mixed by turbulent fluctuations. The mixture fraction model involves the solution for one or two conserved scalars (the mixture fractions). In this approach, the transport equations for individual species are not solved. Instead, the individual component concentrations for the species of interest are derived from the predicted mixture fraction distribution. Physical properties of chemical species and equilibrium data are obtained from the chemical

database. The connection of turbulence and chemistry is derived with the probability density function (PDF), which describes the fraction of time that the fluctuating variable, f takes in a value between f and $f+\Delta f$. The mixture fraction/PDF model is computationally efficient because it does not require the solution of a larger number of species transport equations. This approach has an additional benefit of allowing a more accurate estimation of the flow field mean density than is possible using the finite rate formulation.

Combustor Model

The dimensions of the combustor is approximately 1.47 m in length and 0.74 m in diameter. A full combustor model is shown in Figure 2. The model was developed from three-dimensional data obtained by scanning of the existing combustor in operation. The gas turbine combustor is of the multi-can type and these cans are placed in circumferential arrangement with common centreline. A crossover tubes are connected to each combustor can, which balance the heat evenly among all the cans. It also allows flame propagation between the liners.

FIGURE 2. Combustor liner arrangement in gas turbine

In this work, only a single can is considered for CFD model. A single combustor model considered in this work is shown in Figure 3. It consists of a main burner, diffusion air inlet, secondary air inlet, swirl air inlet, combustor wall, and outlet. Air and natural gas enter the combustor via a swirl burner. At the same time, diffusion air is also channelled to the surrounding cylinder (secondary air), and it serves two purposes: one is for additional air required for complete combustion, and the other is to cool the combustion liner that normally experience high temperature. In order to realistically model the swirl flow prior to fuel-air mixing in the main primary zone, a swirl burner is also modelled. It consists of an array of blocks arranged at specific angle with the reference centre point. Within these blocks, air is injected, creating a swirl-like flow downstream of the burner.

Hybrid mesh (combination of structured and unstructured mesh) was adopted, and this is illustrated in Figure 4. Higher mesh concentration was set in the area of burner region to capture critical flow development in complex geometries.

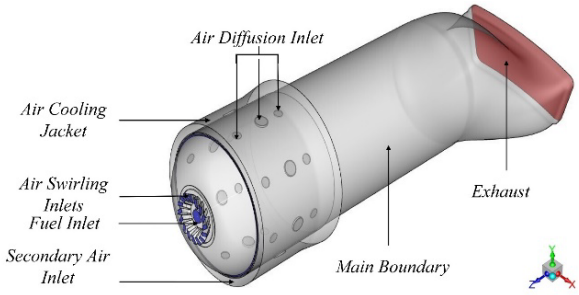

FIGURE 3. Single can-type combustor

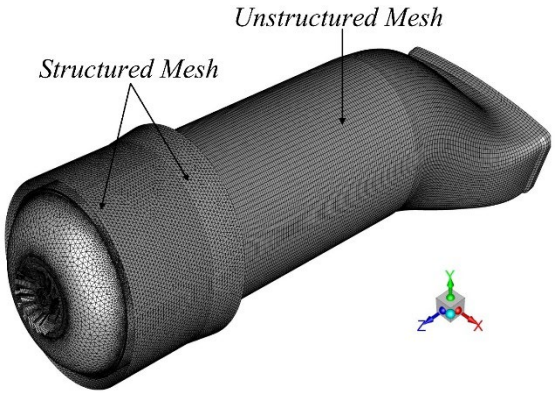

FIGURE 4. Mesh scheme for combustor model

To ensure grid independent solution, few mesh tests were carried out. The flow field and reacting flows are resolved on four different mesh density, namely 0.88, 1.10, 1.32 and 1.52 million cells. Figure 5 shows the temperature profiles along selected planes along combustor length for four different meshes used. The temperature was averaged at each of the planes selected. From this result, it can be said that case with 1.10 million cells is sufficient to resolve the flow field. It is also clear that any further increase in the number of cells gives insignificant changes to the prediction of the exhaust gas temperature. Thus, for the rest of flow and combustion calculation, a grid of 1.10 million cells is used.

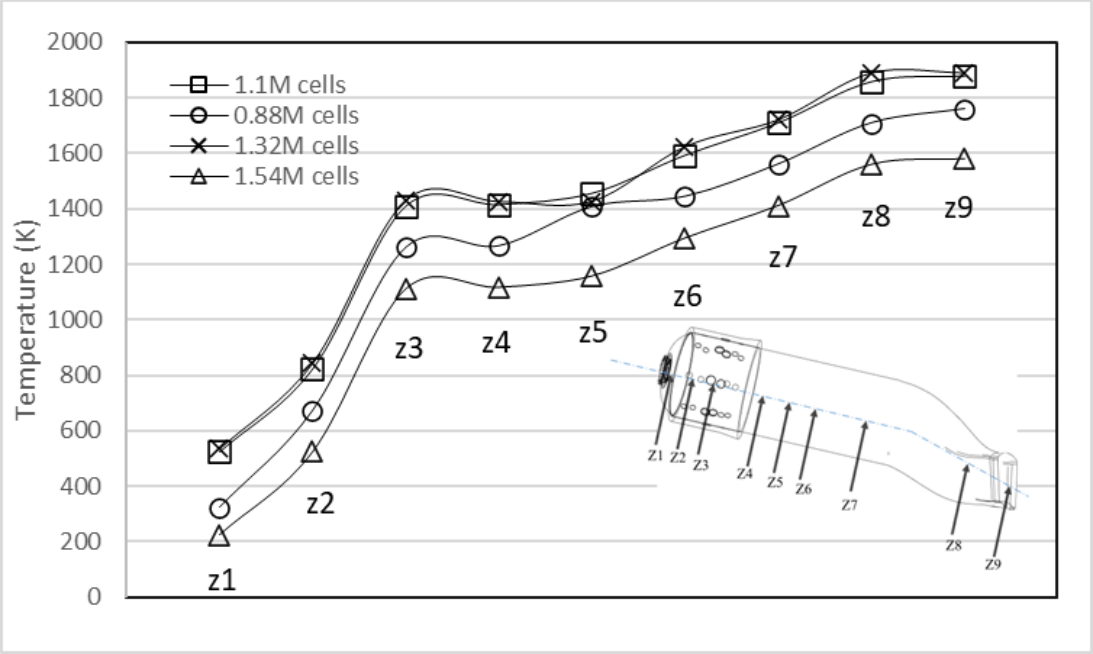

FIGURE 5. Average temperature of exhaust gas on selected planes along combustor length for different mesh density

Model Assumption

In this work, pure methane is assumed as the fuel. Though in reality, natural gas consists of other gas compositions, the amount of these gases is very small and insignificant, i.e., composition of methane is more than 90%. Earlier work has demonstrated that the inclusion of the other gases for numerical investigation did not have any significant difference in the results (Hasini et al., 2013). In this work, focus is given to the effect of excess air supplied to the combustor. The excess air is added to the existing operational condition of a real gas turbine in thermal power plant. The stoichiometric air-fuel ratio was determined to make a good atomic equivalence. The RNG model (Re-Normalisation Group) k-ε is solved for a more realistic closure for turbulence model, that takes into account the complex geometry, swirling effect and separated industrial flows (Toporov et al. 2014).

Boundary Condition

The actual operational data obtained in the power station is taken as the boundary for the simulation. In this case, the air inlet flow rate is set to 21 kg/s, air inlet swirl mass flow rate is 2.7 kg/s, and fuel inlet mass flow rate is 0.48 kg/s. The wall is assumed to be adiabatic since the whole system is well-insulated to prevent any heat from escaping. The outlet is set as a pressure outlet.

Air Fuel Ratio

Table 1 shows the global reaction for the combustion of methane with different sets of excess air. In this investigation, 2.7 kg/s of methane is set as fuel inlet (injected through the primary air swirl burner). 7 different percentage of excess air is systematically simulated in stages. Stoichiometric condition is set as a baseline case, where it corresponds to 0% excess air. Consequently, the mass of primary air is set at 2.83 kg/s for 5% excess air, 2.97 kg/s for 10% excess air, 3.11 kg/s for 15% excess air, 3.24 kg/s for 20% excess air, 3.36 kg/s for 25% excess air, 3.51 kg/s for 30% excess air.

TABLE 1. Fuel Compositions of Methane with excess air

No. of Case	Methane with excess air in percentage	Combustion Equations
Case 1	5%	$CH_4 + 1.05\ a_{th}\ (O_2+3.76\ N_2) \rightarrow CO_2 + 2H_2O + xN_2 + {}_y O_2$
Case 2	10%	$CH_4 + 1.10\ a_{th}\ (O_2+3.76\ N_2) \rightarrow CO_2 + 2H_2O + xN_2 + {}_y O_2$
Case 3	15%	$CH_4 + 1.15\ a_{th}\ (O_2+3.76\ N_2) \rightarrow CO_2 + 2H_2O + xN_2 + {}_y O_2$
Case 4	20%	$CH_4 + 1.20\ a_{th}\ (O_2+3.76\ N_2) \rightarrow CO_2 + 2H_2O + xN_2 + {}_y O_2$
Case 5	25%	$CH_4 + 1.25\ a_{th}\ (O_2+3.76\ N_2) \rightarrow CO_2 + 2H_2O + xN_2 + {}_y O_2$
Case 6	30%	$CH_4 + 1.30\ a_{th}\ (O_2+3.76\ N_2) \rightarrow CO_2 + 2H_2O + xN_2 + {}_y O_2$

RESULTS AND DISCUSSION

Validation

To ensure that the model assumptions used in the simulation are able to yield accurate result for reacting flow, the firing pattern, firing profile, temperature variation, flow rate, pathlines, and vector velocity were calculated. Comparison with actual operational data, as well as from known theoretical values are also made. Due to the fact that the operating condition for combustor is too high, only the temperature of exhaust gas is used for comparison. Also considered was species formation such as O_2, CO_2 and NO_x. Prediction of flame temperature show maximum temperature of about 2400K (2172°C), occurring in the regions circumferenting the centre core at the centre of the flow axis (Hasini et al. 2016). This is relatively high when compared to the operation data during test firing, which indicated flame temperature of between 1871°C to 1935°C. This can be attributed to the fact that in this simulation, pure methane is assumed, whereby, during the actual operation, the gas composition includes other minor gases as well. Also, in reality there are heat losses during combustion that will lower down the maximum flame temperature. Nevertheless, the predicted maximum temperature inside the combustor agrees well with published adiabatic flame temperature for methane, which is 2236 K (1963°C). Deviation from the theoretical flame temperature is approximately 7.3%. Table 2 highlights the comparison made for temperature at with various resources:

TABLE 2. Comparison of exhaust gas temperature with different source, °C. Percentage deviation is made with actual value.

	Gas Temperature, °C	Deviation
Prediction	2172	12.25%
Theoretical	1963	1.45%
Actual (Design)	1871 - 1935	-

Distribution of Temperature Profile in Combustor

Figure 6 shows the flame contour for different excess air. The global range is taken to illustrate the temperature distribution. The temperature is captured at mid plane along the combustor length. The chromatic coloured legend shows the minimum and maximum temperature point in Kelvin. It is noted that the maximum flame temperature occurs in the region surrounding the centre core, and not in the middle of centre core. This is due to the flow of primary swirl air which creates empty hollow region at the centre core. This region is occupied by the fuel upon injection and combustion is initiated at boundaries between the fuel and swirl air. Further downstream, the flame spread, and this can be illustrated by the larger maximum temperature region, before the exit. It is also interesting to see that the difference in flame temperature between all the cases are very small, though the amount of excess air injected into the combustor varies.

Figure 7 shows the temperature contours at several cross-sectional planes along axial distance. The figure compares the velocity contours for different cases of excess air. The development of velocity contours can be observed starting from plane z=0.15m to z=1.45m (from top to bottom). The figures confirm that high temperature regions are located at area circling the centre core for all cases. This formation of this shape is influenced by the high jet velocity of fuel (at centre core) and the swirling jet which divide the flame in two sections from centre core The regions of high temperature tend to be uniform as they progress downstream of the combustor. For Case 1 (without excess air), the high-temperature zones are primarily centred around the first dilution holes along the combustor wall and central axis. With excess air of 5% (Case 2), the contour is almost identical to Case 1, but the temperature is slightly higher. This can also be observed from the plot of temperature profile along combustor length, as shown in Figure 8. Case 3 shows the same two parted profiles, but the temperature is slightly higher than Case 2. Case 4 shows almost identical temperature level as Case 3,while Case 5, and Case 7 shows the same temperature magnitude.

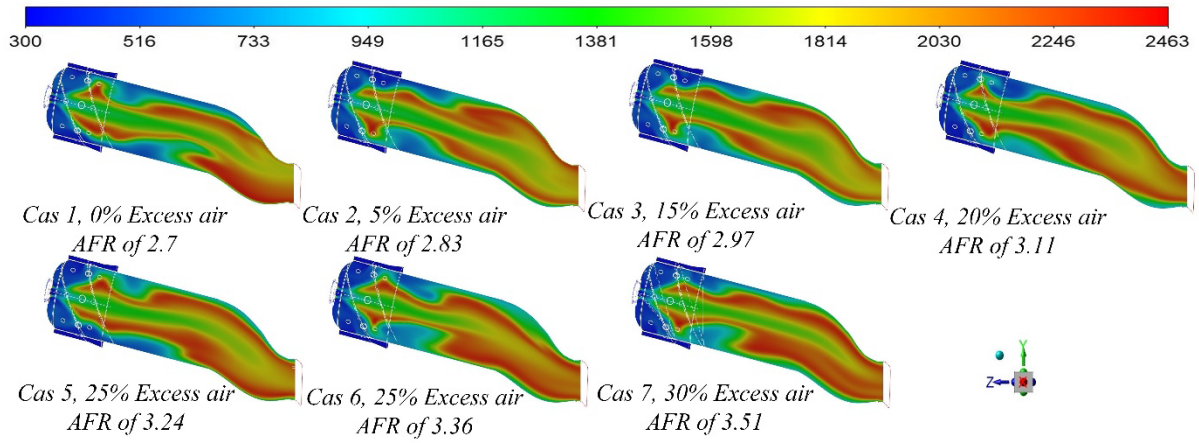

FIGURE 6. Temperature contour and flame profiles for different excess air (in Kelvin)

To ascertain the prediction of temperature along combustor length, a plot of average temperature is made. A few planes were selected as discussed in Figure 7. This time, the weighted average for the temperature is made to represent the average temperature at a given plane. The plot is shown in Figure 8. In general, the average temperature for all cases increases along the combustor length, starting from the burner region at Z1 plant to the outlet, at Z9 plane. Note that the temperature recorded is the average temperature though it is known that the burner region is recording the highest temperature. However, considering that the region covered by this maximum temperature region is small compared to the regions of lower temperature. This results in the average temperature being relatively low compared to downstream planes. From the plot it is also clear that the amount of excess air does not have significant impact to the average temperature of the exhaust gas in the combustor.

	Temperature profile for different AFR kg/s						
The point at Z plane distance (m)	*2.7*	*2.83*	*2.97*	*3.11*	*3.24*	*3.36*	*3.51*
0.15	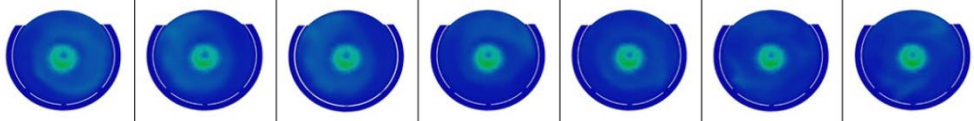						
0.25	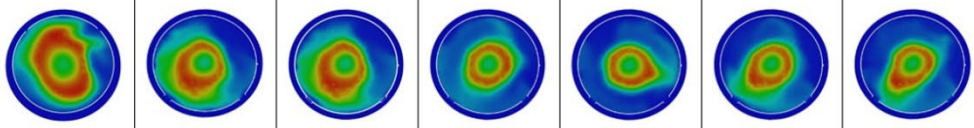						
0.50	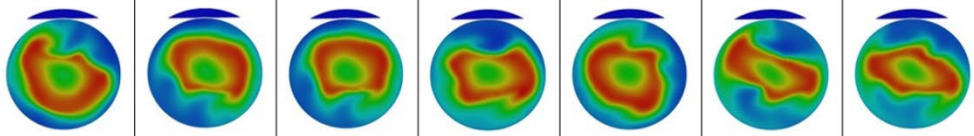						
0.75	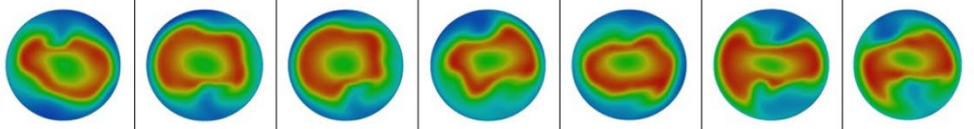						
0.95	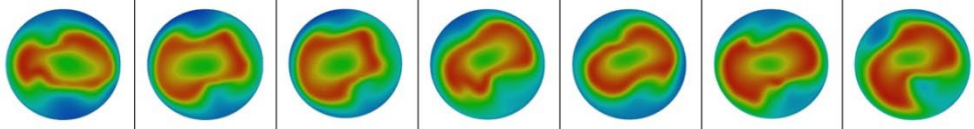						
1.05	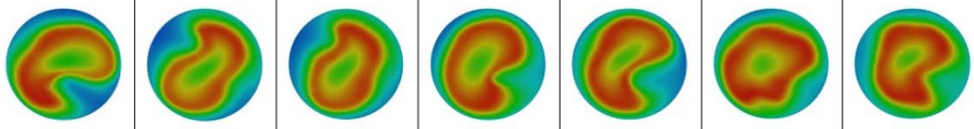						
1.15	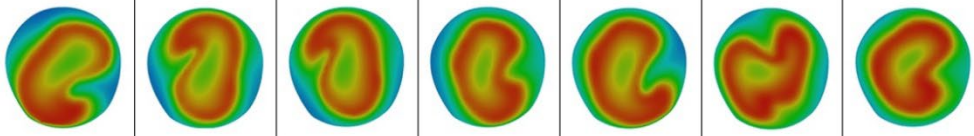						
1.35	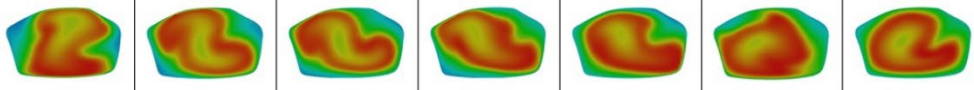						
1.45	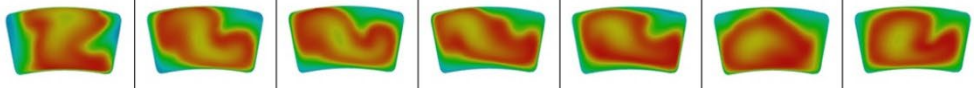						

FIGURE 7. Average temperature at several cross-sectional planes along axial direction

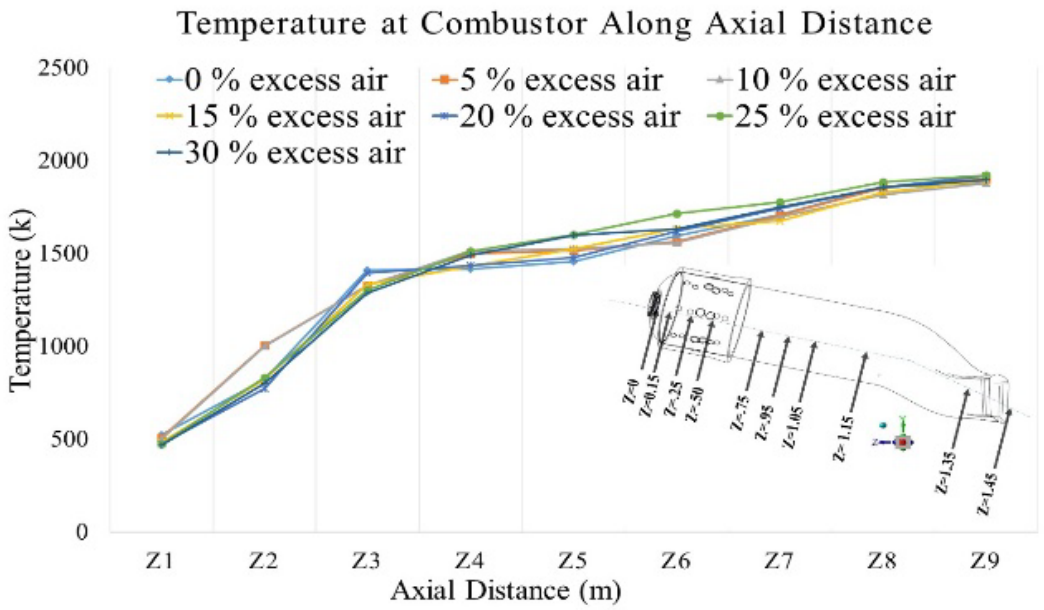

FIGURE 8. Average temperature at several cross-sectional planes along axial direction

Velocity Profile

Figure 9(a) illustrates the pathline for fuel starting from the inlet port injection to the combustor exit. Fuel enters the combustor and reacts with swirl air that enters via swirl nozzle. Chemical reaction occurs at the interface between both mixtures and proceeds downstream. Figure 9(b) represents the contours of velocity where the distribution of fuel-air mixture in seven different cases show identical pattern. For all cases, the fuel is consumed within the combustor primary zone, indicating good mixing of air and fuel. The velocity of exhaust gas ranges from 0 m/s (at recirculation zone) to 160 m/s at nozzle jet.

The recirculation zone can also be observed from Figure 9(c). The recirculation zone forms due to fast jet velocity of fuel and air in the centre core. At the same time, residual air/fuel that departs from the centre flow radially outwards and some mixture closed to the wall flow in the reverse direction. The impact forms a recirculation zone in the outer area of the main combustion zone. Magnified view of this recirculation zone shown in Figure 10. The velocity vector represents the position and direction of the air fuel mixture post-firing, and it is noted that the vector in axial direction downstream of the main combustion zone is uniform.

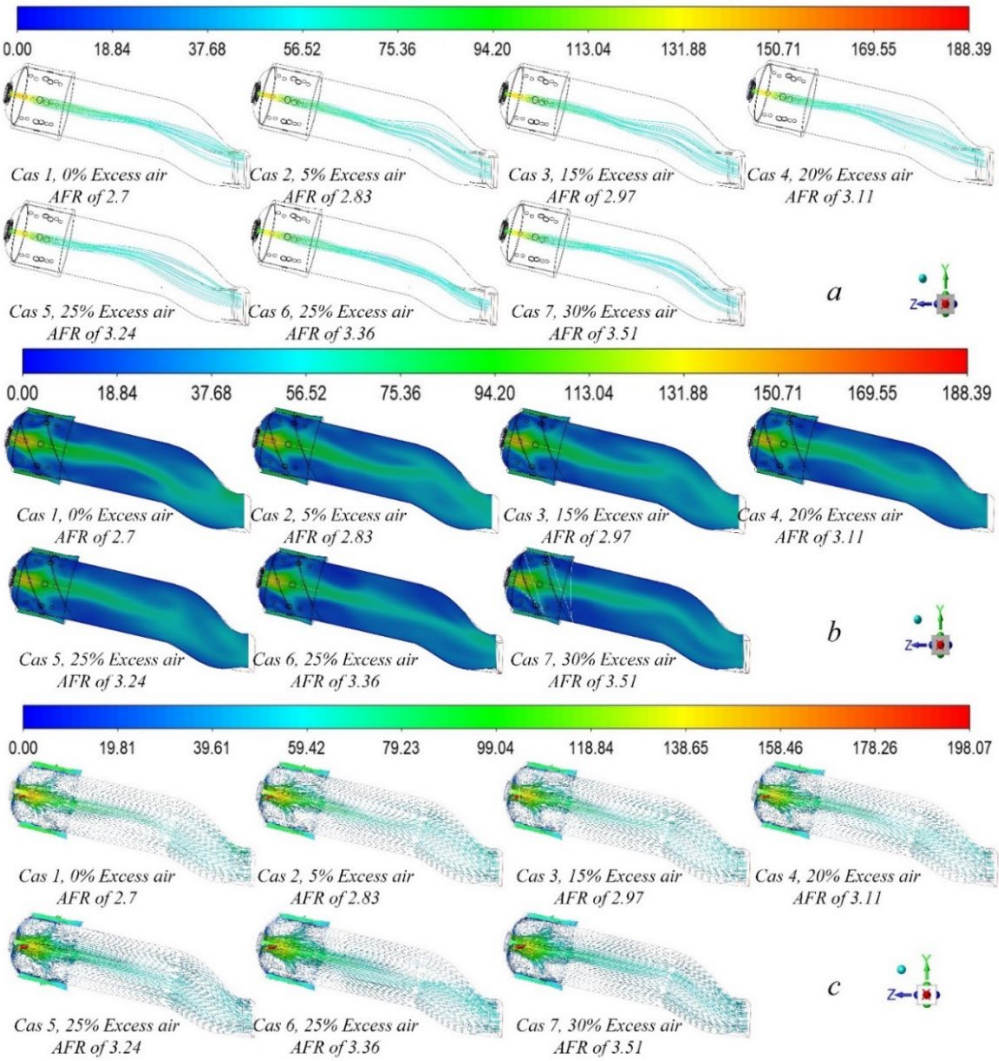

FIGURE 9. (a) Pathlines, (b) velocity contours and (c) velocity vector of combustion gas (unit in m/s)

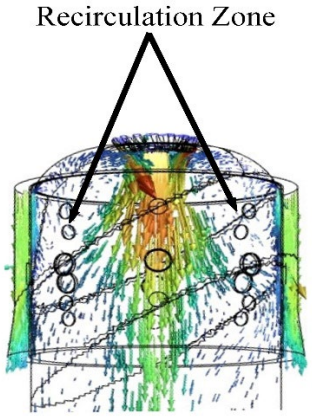

FIGURE 10. Turbulent flow and recirculation zone

Distribution of CO_2 and O_2

The distribution of CO_2 at combustor mid plane for different excess air cases are shown in Figure 11. CO_2 is at maximum in the regions where temperature is maximum, indicating complete combustion. For the CO_2 distribution at mid plane, there is small difference between cases of different excess air. However, at the outlet of combustor, the CO_2 content varies significantly between cases. As shown in Figure 12, 5% and 25% excess air gives the highest CO_2 emission, while the lowest CO_2 is given when excess air is 10%. There is no exact relation that can be derived from the effect of excess air to the production of CO_2. It is known that excess air is injected into the combustor to increase the chances of getting complete combustion. The prediction of CO_2 agrees very well with the practice of gas turbine owners, which usually set 20-25%

excess air during normal operation. This corresponds to the maximum CO_2, which directly implies complete combustion.

Apart from CO_2, another indicator commonly used to gauge the performance of combustion in gas turbine combustor is the mass fraction of O_2. The prediction of O_2 concentration at mid plane and at the exit are shown in Figure 13 and Figure 14, respectively. At mid plane, the distribution of O_2 for all cases of different excess air shows relatively identical trend. It can be observed that O_2 is fully consumed in the centre core region. Further downstream, the region of "zero" O_2 increases, indicating that combustion reaction is still occurring beyond the main combustion region. High concentration of O_2 is predicted in the region where flow recirculation is. This is considered as a dead zone where no fuel is expected to flow within this region, thus there is no combustion. Quantitatively, no clear trend for O_2 concentration can be deduced for different excess air cases. For all the cases, the percentage excess air ranges from 4.3% to 4.8%. Highest excess air case gives the highest O_2 concentration at the outlet (4.8% O_2). Interestingly, it is shown that the Case of 5% excess air gives the lowest O_2 concentration at the outlet (4.3% O_2).

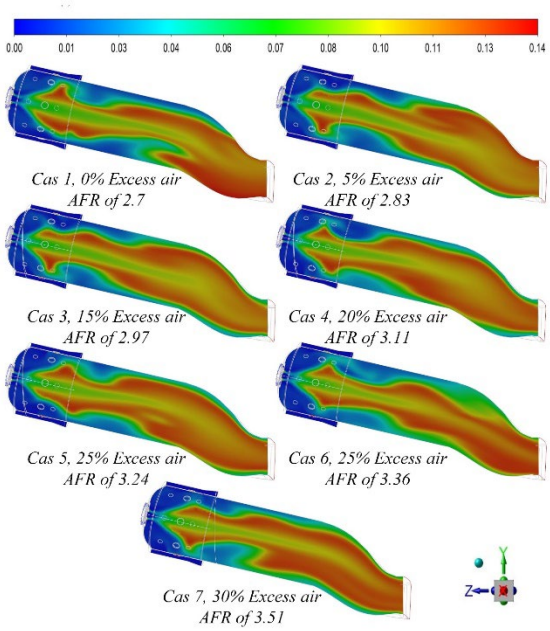

FIGURE 11. Mass fraction of CO_2 profile

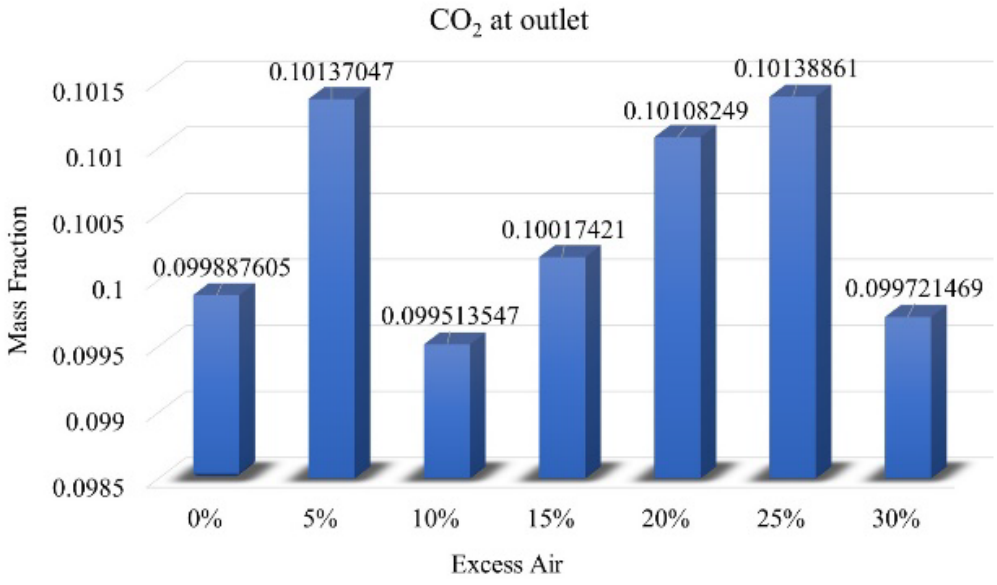

FIGURE 12. Mass fraction level of CO_2

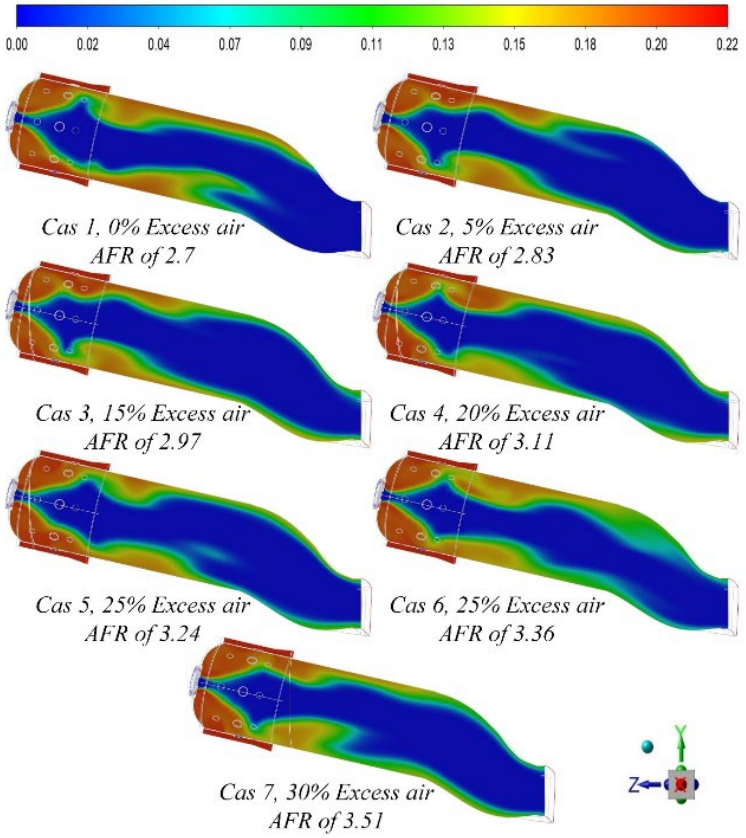

FIGURE 13. Mass fraction of O_2 profile

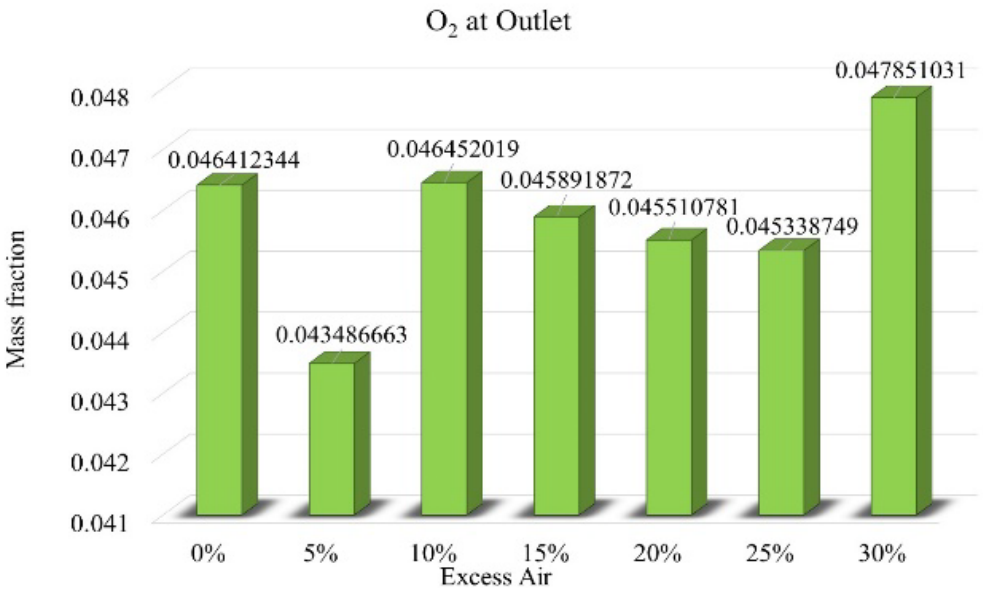

FIGURE 14. Mass fraction level of O_2

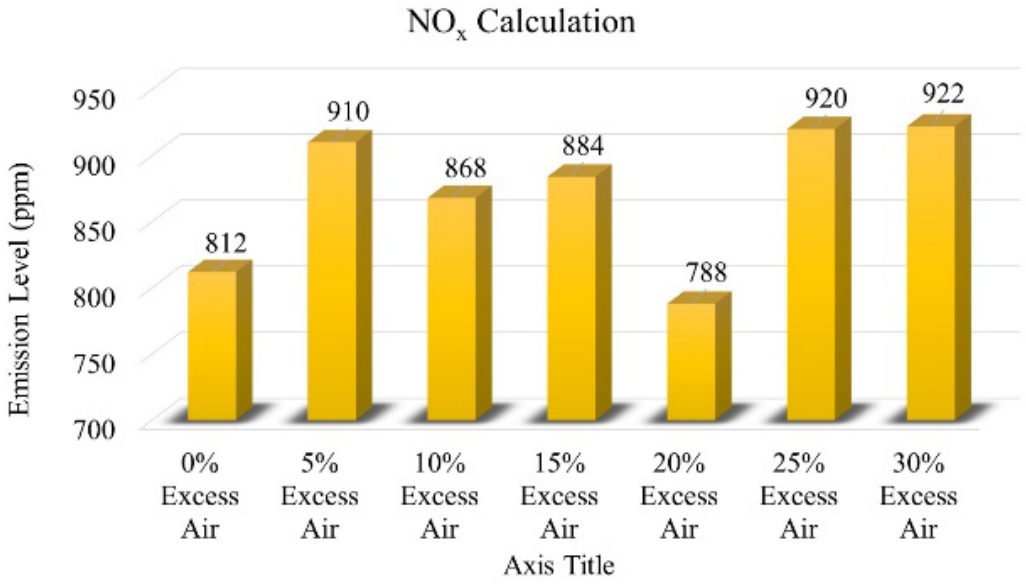

FIGURE 15. Contour of local NO_x distribution at combustor outlet (ppm)

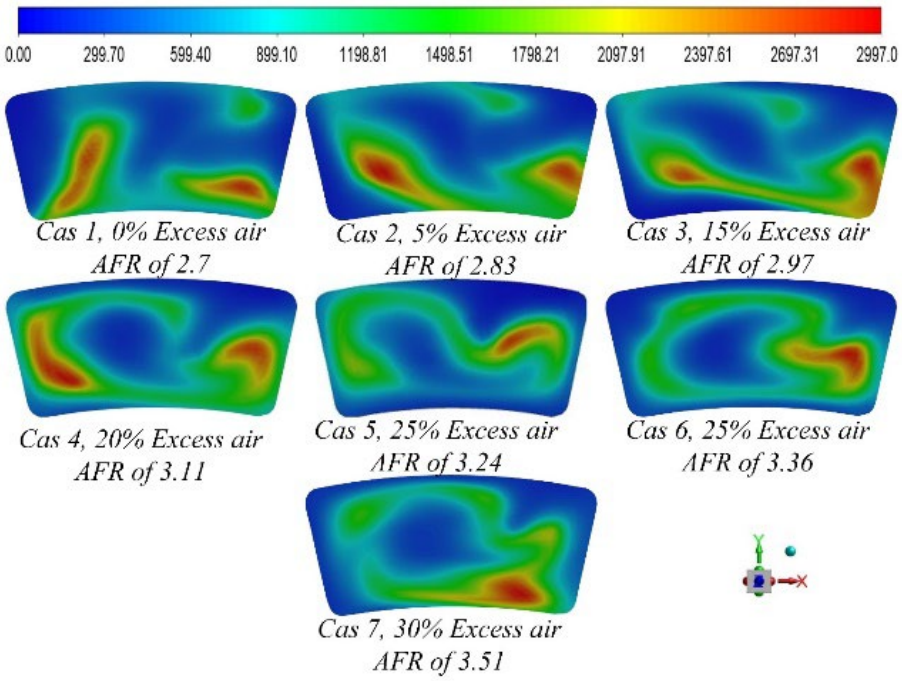

FIGURE 16. Quantitative prediction of NO_x at varying excess air

Effect of Excess Air to NO_x Production

The contours of NO_x at combustor exit for different excess air cases are illustrated in Figure 15. Spots of the highest NO_x concentration are visible in some locations at the combustor exit planes. The maximum dynamics ppm of NO_x is about 2820 ppm, which is considered very high. This can be attributed to the fact that even at the combustor exit regions, the exhaust gas temperature is still very high and they are scattered in specific spots in the exit planes. It is known that NO_x production is a strong function of the temperature. It is also noted that these spots can be estimated to cover less than 5% of the overall cross-sectional area of the exit plane. Most of the regions are dominated by zero NO_x presence. Therefore, to represent NO_x distribution more accurately at the combustor exit, a weighted average value of this species is calculated and this is presented in Figure 16. It is interesting to observe that there is no specific trend between the net NO_x at combustor exit and the percentage of excess air. The

highest NO_x is observed when the excess air ratio is the highest at 30%, followed by 25% and 5%, while the lowest NO_x is given when the excess air is at 20% and 0%. It can be said that at the combustor exit, the reaction of NO_x with its surrounding radicals is still ongoing due to higher surrounding temperature. It is also expected that the reaction will still continue as combustion gas flows downstream towards the gas turbine sections until the turbine outlet. As such, it is also expected that the NO_x concentration will further reduce.

CONCLUSION

CFD simulation on the effect of excess air to the combustion characteristics, temperature distribution, velocity profile and emissions in a full-scale gas turbine combustor was carried out. Real operating data of gas turbine combustor was used as the boundary conditions. Different excess air amount was systematically tested, namely stoichiometric, 5%, 10%, 15%, 20%, 25% and 30%. The predicted adiabatic flame temperature is compared with plant design data and reasonable agreement was obtained. The difference in the predicted temperature was attributed to the fact that in the simulation, 100% CH_4 is assumed while in the real operating data, the composition of the natural gas varies slightly. Based on the simulation, the following conclusions can be withdrawn:

1. The excess air ratio has insignificant effect to the velocity and temperature distribution inside the combustor. The general flow show that fuel and air are highly mixed in the main combustor region and the velocity becomes uniform downstream of the combustor.
2. Distribution of emissions, i.e. CO_2 and O_2 at combustor mid and exit planes are highly influenced by the amount of excess air used. High composition of CO_2 is predicted at the location where the exhaust gas temperature is the highest.
3. At the combustor exit, 25% excess air give the highest CO_2 emission, due to the fact that this ratio is optimum to ensure complete combustion. Fuel is completely burned, thus resulting in high amount of CO_2.
4. The amount of O_2 at combustor exit for all excess air cases does not differ much. It ranges from 4.3% to 4.8%. Higher excess air results in the higher O_2 concentration at combustor exit.
5. The excess air ratio has no significant impact to NO_x production in gas turbine combustor. Instead, it is highly influenced by the temperature of exhaust gas during and after combustion.

ACKNOWLEDGEMENT

The authors would like to acknowledge the financial support received from UNITEN-Universitas Pertamina Matching Grant (2022003YCUPU) that enables to work to be completed.

DECLARATION OF COMPETING INTEREST

None

REFERENCES

Abdul Rahman, M.R., Wan Shuin, W.M.A., Saad, M. R., Che Idris, A., Mohd Faizal, H., "Combustion Characteristics inside Micro Channel Combustor", Jurnal Kejuruteraan S1 4(1) 2021: 109-116.

Beddu, S., Abd Manan, T.S., Mohd Zainoodin, M., Mohd Kamal, N.L., Machmudah, A., Yavari, S., Mohamad, D., Itam, Z., Syamsir, A., Mohamed Nazri, F., Yee, H.M., Ahmad Zailani, W.W., Mohd Yapandi, M.F.K., Che Muda, Z., Ghanim, A.A.j., Isa, M.H., Shafiq, N., Ahmad, A., Wan Rasdi, N. "Characterization of Cenospeheres from Malaysian Coal Generated Power Plants: Jimah, Kapar and Manjung". Jurnal Kejuruteraan, 34(6) 2022: 1251-1264.

Ezekiel Enterprises, LLC. "Fundamentals of Gas Turbine Engines NONRESIDENT TRAINING Technician (Electrical) 3 / Gas," no. 3923 (2015). https://d6s74no67skb0.cloudfront.net/course-material/ME925-Fundamentals-of-Gas-Turbine-Engines.pdf.

Ghenai, Chaouki. "Combustion of Syngas Fuel in Gas Turbine Can Combustor." *Advances in Mechanical Engineering* 2010 (2010). https://doi.org/10.1155/2010/342357.

Hasini, H., Shuaib, N.H., Fahmi, Abdullah, W.A.F.W., "CFD Analysis of Temperature Distribution in Can-Type Combustor Firing Synthetic Gas" Applied Mechanics and Materials, 393 (2013), pp. 741-746.

Hasini, H., S. S.A. Fadhil, N. Mat Zian, and Ni Om. "CFD Investigation of Pollutant Emission in Can-Type Combustor Firing Natural Gas, LNG and Syngas." *IOP Conference Series: Earth and Environmental Science* 32, no. 1 (March 2016): 012073. https://doi.org/10.1088/1755-1315/32/1/012073.

Houghton, JT; Jenkins, GJ; Ephraums, JJ. "US Department of Energy Office of Scientific and

Technical Information .” Nucl. Phys., 1990. https://www.osti.gov/biblio/200217.

Jiang, Yu, M. Barzegar Gerdroodbary, M. Sheikholeslami, Houman Babazadeh, Ahmad Shafee, R. Moradi, and Zhixiong Li. “Influence of Upstream Strut on Hydrogen Fuel Distribution inside the Supersonic Combustion Chamber.” *International Journal of Hydrogen Energy* 45, no. 41 (August 2020): 22032–40. https://doi.org/10.1016/j.ijhydene.2020.06.026.

Jiang, Yu, Masoud Hajivand, H. Sadeghi, M. Barzegar Gerdroodbary, and Zhixiong Li. “Influence of Trapezoidal Lobe Strut on Fuel Mixing and Combustion in Supersonic Combustion Chamber.” *Aerospace Science and Technology* 116 (September 2021): 106841. https://doi.org/10.1016/j.ast.2021.106841.

Li, Chengqin, Xinyu Li, and Desan Guo. “Experimental Study of a Low Calorific Value Combustor for Micro Gas Turbine.” In *Zhongguo Dianji Gongcheng Xuebao/Proceedings of the Chinese Society of Electrical Engineering*, 39:5829–34, 2019. https://doi.org/10.13334/j.0258-8013.pcsee.190071.

Liu, C. Y., G. Chen, N. Sipöcz, M. Assadi, and X. S. Bai. “Characteristics of Oxy-Fuel Combustion in Gas Turbines.” *Applied Energy* 89, no. 1 (January 2012): 387–94. https://doi.org/10.1016/j.apenergy.2011.08.004.

Mahmoud, Rihab, Mehdi Jangi, Benoit Fiorina, Michael Pfitzner, and Amsini Sadiki. “Numerical Investigation of an Oxyfuelnon-Premixed Combustion Using a Hybrid Eulerian Stochastic Field/Flamelet Progress Variable Approach: Effects of H2/CO2 Enrichment and Reynolds Number.” *Energies* 11, no. 11 (November 2018): 3158. https://doi.org/10.3390/en11113158.

Nemitallah, By M A, and M A Habib. “Numerical Investigations of Methane Fueled Oxy-Fuel Combustion Model in a Gas Turbine Combustor 1 . Flow Fields , Temperature , and Species Distribution 2 . Effect of CO 2 Recirculation 1 Introduction 2 Numerical Modeling,” n.d., 92–98.

Okafor, Ekenechukwu C., K. D. Kunkuma A. Somarathne, Rattanasupapornsak Ratthanan, Akihiro Hayakawa, Taku Kudo, Osamu Kurata, Norihiko Iki, Taku Tsujimura, Hirohide Furutani, and Hideaki Kobayashi. “Control of NOx and Other Emissions in Micro Gas Turbine Combustors Fuelled with Mixtures of Methane and Ammonia.” *Combustion and Flame* 211 (January 2020): 406–16. https://doi.org/10.1016/j.combustflame.2019.10.012.

Shakeel, Mohammad Raghib, Yinka S. Sanusi, and Esmail M.A. Mokheimer. “Numerical Modeling of Oxy-Methane Combustion in a Model Gas Turbine Combustor.” *Applied Energy* 228 (October 2018): 68–81. https://doi.org/10.1016/j.apenergy.2018.06.071.

Smith, Gregory P. Golden, David M., Frenklach, Michael, Moriarty, Nigel W., Eiteneer, Boris, Goldenberg, Mikhail C. Bowman Thomas, Hanson, Ronald K., Soonho Song, Gardiner, Jr., William C., Lissianski, Vitali V. and Qin Zhiwei, http://combustion.berkeley.edu/gri-mech/

Prasanna Kumar, T.J., S Koteswara Rao, S Durga Prasad, and Md Faisal, P Anil. “Design Optimization of Can Type Combustor.” *International Journal of Engineering Research And* V5, no. 11 (2016): 66–73. https://doi.org/10.17577/ijertv5is110085.

Tamang, Sajan, and Heesung Park. “Numerical Investigation of Combustion Characteristics for Hydrogen Mixed Fuel in a Can-Type Model of the Gas Turbine Combustor.” *International Journal of Hydrogen Energy*, June 2022. https://doi.org/10.1016/j.ijhydene.2022.05.273.

Tian, Zhenyu, Yuyang Li, Lidong Zhang, Peter Glarborg, and Fei Qi. “An Experimental and Kinetic Modeling Study of Premixed NH3/CH4/O2/Ar Flames at Low Pressure.” *Combustion and Flame* 156, no. 7 (July 2009): 1413–26. https://doi.org/10.1016/j.combustflame.2009.03.005.

Toporov, Dobrin D. “Mathematical Modelling and Model Validations.” In *Combustion of Pulverised Coal in a Mixture of Oxygen and Recycled Flue Gas*, 51–97. Elsevier, 2014. https://doi.org/10.1016/b978-0-08-099998-2.00004-7.

Wang, Yunyun, Liu Jiang, Luyu Wang, Zaiguo Fu, and Peifen Weng. “Non-Premixed Combustion and Nox Emission Characteristics in a Micro Gas Turbine Swirl Combustion Chamber Fueled by Methane and Ammonia at Different Heat Loads.” *SSRN Electronic Journal* 9, no. 3 (March 2022): e14521. https://doi.org/10.2139/ssrn.4054243.

Woo, Mino, Byung Chul Choi, and Ahmed F. Ghoniem. “Experimental and Numerical Studies on NOx Emission Characteristics in Laminar Non-Premixed Jet Flames of Ammonia-Containing Methane Fuel with Oxygen/Nitrogen Oxidizer.” *Energy* 114 (November 2016): 961–72. https://doi.org/10.1016/j.energy.2016.07.150.

Xiao, Yinli, Zhibo Cao, and Changwu Wang. “The Effect of Dilution Air Jets on Aero-Engine Combustor Performance.” *International Journal of Turbo and Jet Engines* 36, no. 3 (August 2019): 257–69. https://doi.org/10.1515/tjj-2018-0045.

Yan, Yunfei, Wei Gao, Hongyan Guo, Hongyu Yan, Kaiming Shen, Li Zhang, and Zhongqing Yang. “Catalytic Combustion Characteristics of CH4 in the Micro Cavity-Combustor under Different Types of Air Inlet Distribution.” *International Journal of Energy Research* 45, no. 3 (March 2021): 3870–82. https://doi.org/10.1002/er.6039.

Zeng, Wen, Liyao Pang, Weilin Zheng, and Erjiang Hu. “Study on Combustion and Emission Characteristics of a Heavy-Duty Gas Turbine Combustor Fueled with Natural Gas.” *Fuel* 275 (September 2020): 117988. https://doi.org/10.1016/j.fuel.2020.117988.